Electronic Supplementary Information (ESI)

Large scale application of immobilized enzymes call for a change of paradigm: exploring rice husk as viable renewable alternative to organic resins.

L. Corici[a,e], V. Ferrario[b], A. Pellis[b,d], C. Ebert[b], S. Lotteria[b], S. Cantone[a,f], D. Voinovich[b], L. Gardossi[b,c]

a. *SPRIN S.p.a., Via Flavia 23/1, 34148, Trieste, Italy*
b. *Laboratory of Applied and Computational Biocatalysis, Dipartimento di Scienze Chimiche e Farmaceutiche, Università degli Studi di Trieste, Piazzale Europa 1, 34127, Trieste, Italy*
c. *Corresponding author: prof. Lucia Gardossi: gardossi@units.it*
d. *Current address: University of Natural Resources and Life Sciences, Vienna, Department for Agrobiotechnology IFA-Tulln, Institute for Environmental Biotechnology, Konrad Lorenz Strasse 20, A-3430 Tulln an der Donau, Austria.*
e. *Current address: Institute of Chemistry Timisoara of Romanian Academy, Mihai Viteazul 24, 300223 Timisoara, Romania*
f. *Current address: Università degli Studi di Trieste, Piazzale Europa 1, 34127, Trieste, Italy*

Electronic Supplementary Information (ESI) available: [details of any supplementary information available should be included here]. See DOI: 10.1039/x0xx00000x

Figure S1: Sample preparation for chemical analysis.

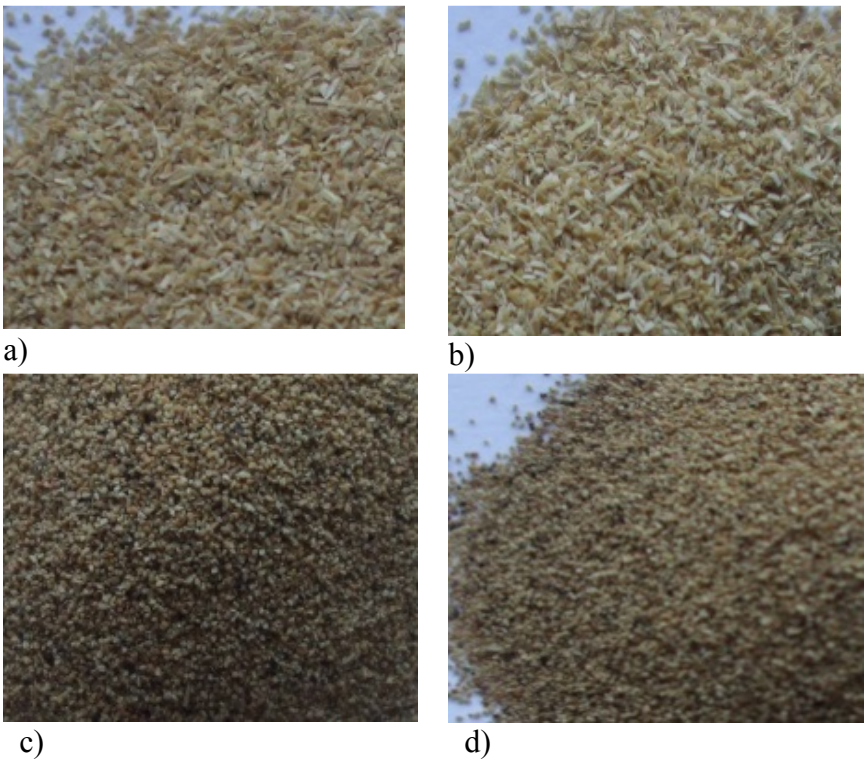

Figure S2. Photographs of rice husk and nut shell: (a) untreated rice husk, (b) extractive-free rice husk, (c) untreated nut shell, and (d) extractive free nut shell.

Table S1. Comparison of major organic chemical components of rice husk and nut shells after extractive treatments.

Composition (%wt)	Rice husk (acetone/H_2O extraction)	Nut shell (toluene/ethanol extraction)
Moisture	8.2	6.0
Cellulose	46.5	29.3
Lignin	31.9	32.4
Pentosans	22.1	21.3

S3. Spectroscopic characterization *via* FT-IR.

The FT-IR spectra of rice husk and nut shell are characterized by a dominant -OH stretch band (ca. 3500-3000 cm^{-1}) attributed to cellulose and hemicelluloses and lignin. A broad absorption at 1730-1710 cm^{-1} in the spectra is ascribable to the acetyl and uronic ester groups of the hemicellulose. A shoulder at 1731 cm^{-1} (RH) is resolved in nut shell spectra and can be assigned to lignin. A band at 1653 cm^{-1} band can be recognized as the ester linkage of carboxylic group of the ferulic and p-coumaric acids of lignin and/or hemicelluloses. The aromatic C=C stretch from aromatic ring of lignin gives two peaks at 1600 and 1504 cm^{-1}. The region of 1200-1000 cm^{-1} represents the C–O stretch and deformation bands in cellulose, lignin and residual hemicelluloses. A small sharp band at 893 cm^{-1}, which is indicative of the C-1 group frequency or ring frequency, is characteristic of β-glycosidic linkages between the sugar units in amorphous cellulose. Absorbances at 1270, 1156, 1075 and 896 cm^{-1} are associated with the typical values of cellulose and are more prominent in the spectrum of rice.

The peak near 3650-3200 cm^{-1}, in both spectra, is representative for OH stretching. A broad absorption was observed around 1730-1710 cm^{-1} in the spectrum corresponding to the rice husk is ascribed to C=O stretching of acetyl and ester groups in hemicellulose and lignin. The band at 1651 cm^{-1} can be recognized as the ester linkage of carboxylic groups in ferulic components of hemicellulose. A shoulder at 1731 cm^{-1} (ascribed to lignin) is more pronounced in nut shell. The existence of this peak was also reported by Alemdar and Sain[1] and Sun et al.[2] for untreated wheat straw.

Some characteristic peaks of cellulose can be observed at 1650 cm^{-1} corresponding to OH bending of adsorbed water in cellulose structure. On the other hand, the vibrations of the aromatic rings can be seen at 1592 and 1504 cm^{-1}, which can be only related to lignin.

The absorption phenomenon around 1270 cm^{-1} refers to the bending frequency of C-O, while the absorption around 890 cm^{-1} observed in both spectra refers to the CH deformation vibration in cellulose[1]. The inorganic part (silica) is characterised by the peaks at in the range of 1100-1070 and 965 cm^{-1}.

Morphological characterisation of rice husk and nut shells by scanning electron microscopy

Scanning electron microscopy (SEM) using a model Philips XL 30 was used to observe the surface morphology of the rice husk fibres.

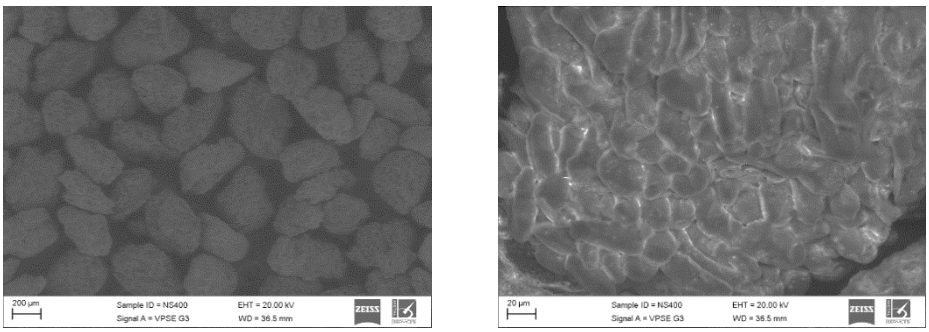

Figure S4. Scanning electron micrographs of milled nut shell at different orders of magnification

Plot on graph paper absorbance against milligrams of xylan.

Xylose (mg)	Xylan (mg)	Absorbance (630 nm)
59.9	52.712	0.1093
102.7	90.376	0.1561
208.5	183.48	0.3085

[1] Alemdar A., Sain M., 2008. Isolation and characterization of nanofibers from agricultural residues – Wheat straw and soy hulls. *Bioresour. Technol*. 99, 1664–1671

[2] Sun, X.F., Xu, F., Sun, R.C., Fowler, P., Baird, M.S., 2005. Characteristics of degraded cellulose obtained from steam-exploded wheat straw. *Carbohydr. Res*. 340, 97–106

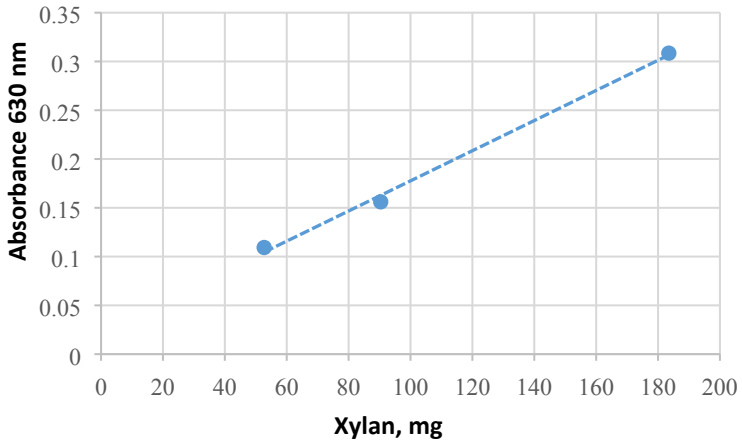

Figure S5. Calibration for the: absorbance (630 nm) *vs* amount of xylan (mg).

Polycondensation of DMA with BDO catalyzed by CaLB immobilized on commercial EC-EP/S.
The DMA (35 mmol) and the diol (BDO, 35.8 mmol) were mixed in a round bottom flask and the biocatalyst, 10% w w^{-1} with respect to the total amount of monomers, Epox-CaLB (activity of about 2000 U g_{dry}^{-1}) was added. The reaction was carried out for 24 h at 50 °C on thin film at reduced pressure (70 mmHg).

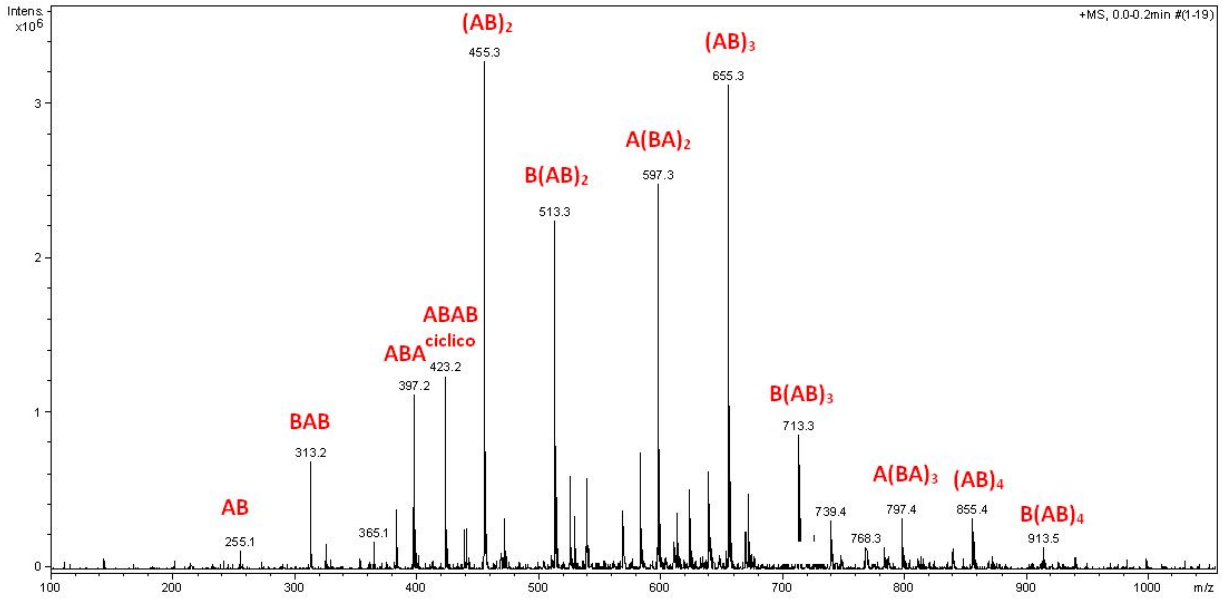

Figure S6. ESI-MS positive ion mass spectrum of polycondensation product of DMA (A) with BDO (B) catalyzed by Epox-CALB 10% w w^{-1} with respect to the total amount of monomers, Epox-CaLB (activity of about 2000 U g_{dry}^{-1}) at 50 °C on thin film at reduced pressure (70 mmHg). Conversion: 87%.

The conversion of the reactions was monitored by exploiting the ^{1}H-NMR of protons of methylene group adjacent to ester moiety (signals in the range of ~ 3.8-4.0 ppm (d)) and the signals at δ=2.24 of methylene protons (b) (-CH_2-CH_2-C(O)O-, the latter assumed constant throughout the reaction). The formation of the oligomers is confirmed by the signals of protons of residual methyl group. Methylenic protons (c) of DMA give signals at 1.58 ppm.

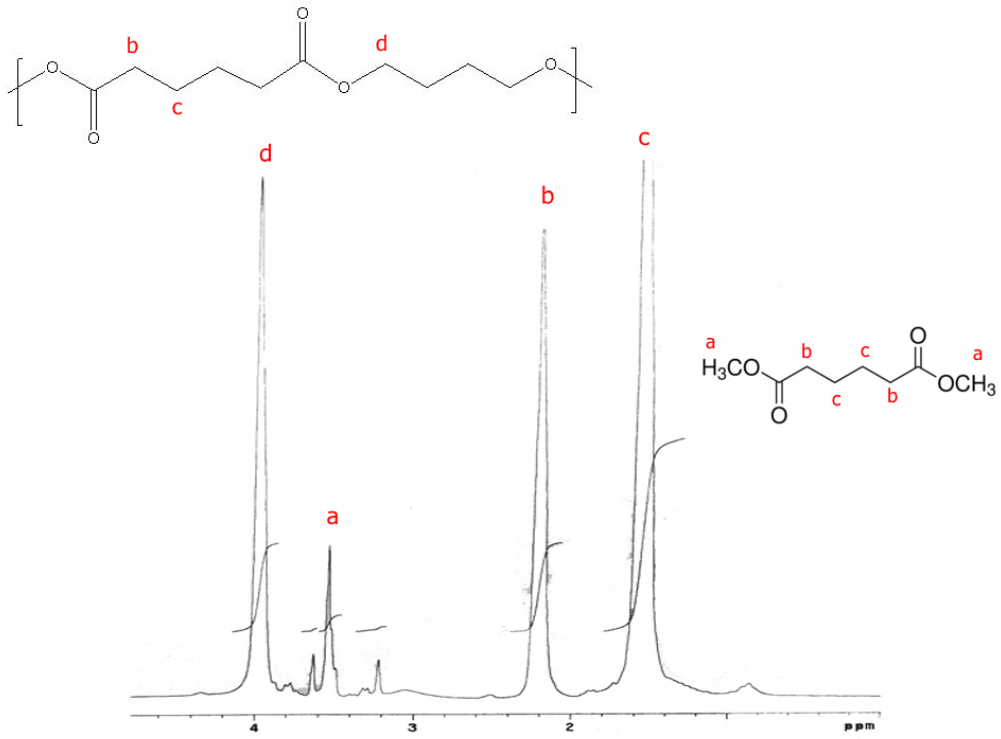

Figure S7. ^{1}H-NMR spectrum of P(BA) synthesized using CaLB on EC-EP/S.
^{1}H-NMR ($CDCl_3$), δ 4.0 (2H, t, CH_2-CH_2-O-CO-), 3.61 (3H, s, CH_2-CO-OCH_3), 3.49 (2H, t, -CH_2-CH_2-OH), 2.24 (2H, t, -CH_2-CH_2-CO-), 1.58 (2H, quintet, -CH_2-CH_2-CH_2-).

Polycondensation of DMA and BDO catalyzed by RH-CaLB

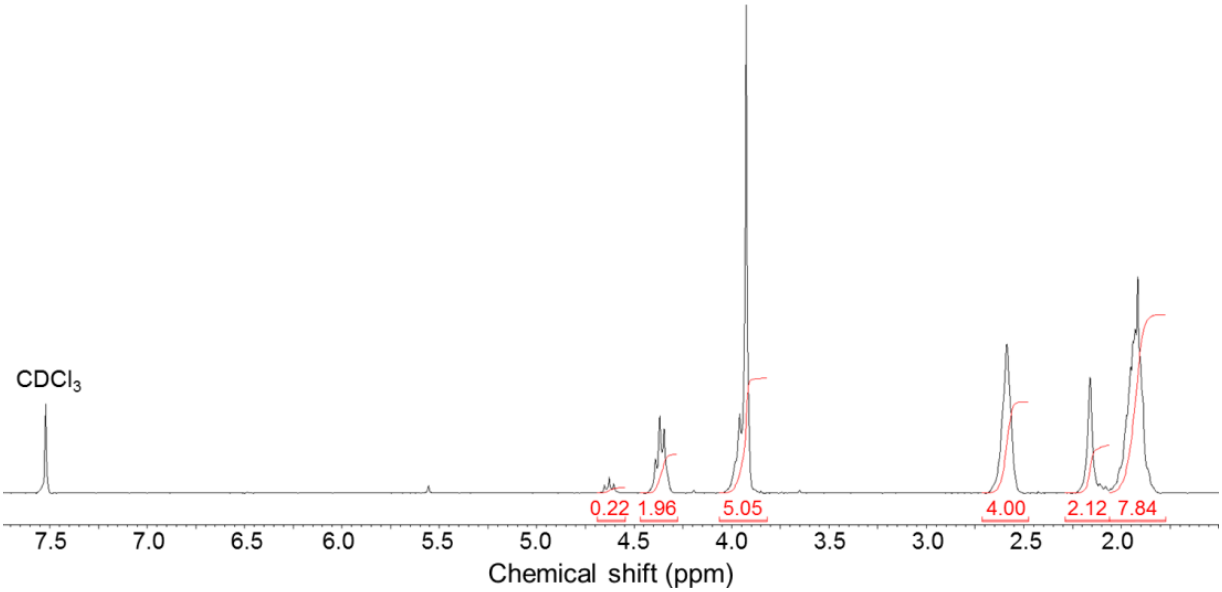

Figure S8. ^{1}H-NMR spectrum of the polycondensation products of DMA with BDO catalyzed by 10% w/w dry RH-CaLB at 24 h and 1000 mbar. Conversion: 42%.

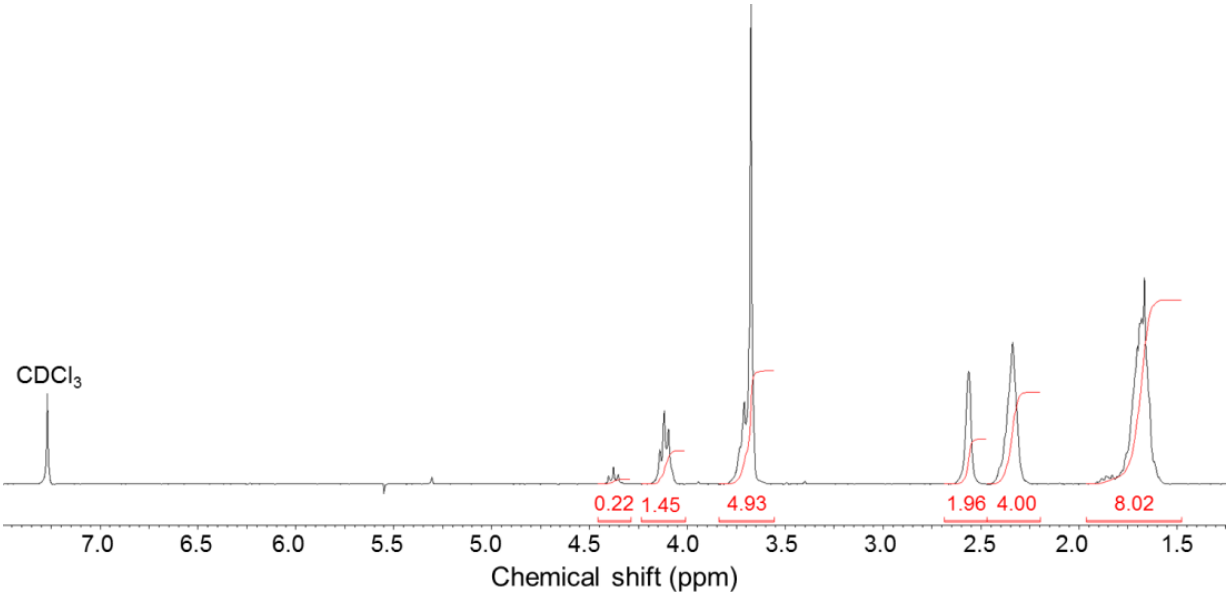

Figure S9. [1]H-NMR spectrum of the polycondensation products of DMA with BDO catalyzed by 10% w/w wet RH-CaLB at 24 h and 1000 mbar. Conversion: 36%.

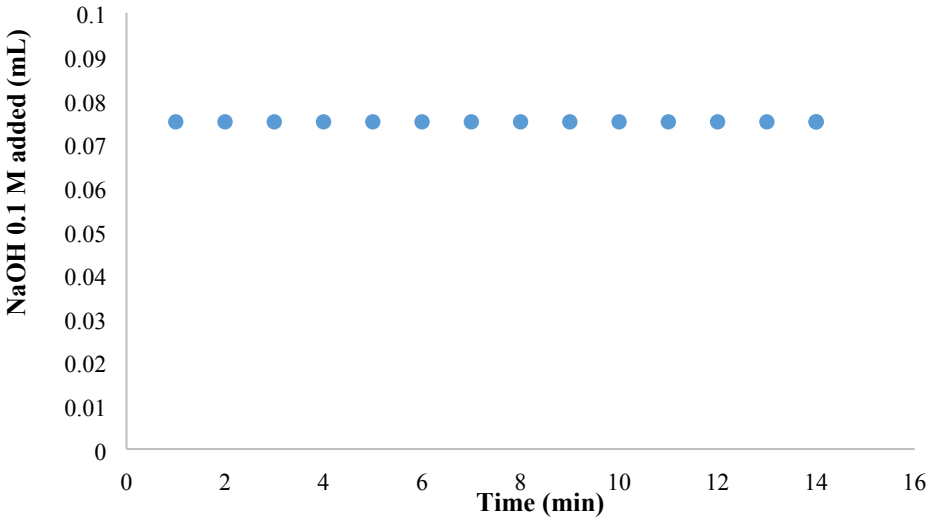

Figure S10. Titration of residual activity present in the aqueous mixture used for hydrolytic assay of covalently immobilized RH-CaLB . Titration was carried out after 14 min incubation under stirring at 30°C and upon filtering of the immobilized biocatalyst. The graphic confirms that no free active enzyme leached off the support during the assay.

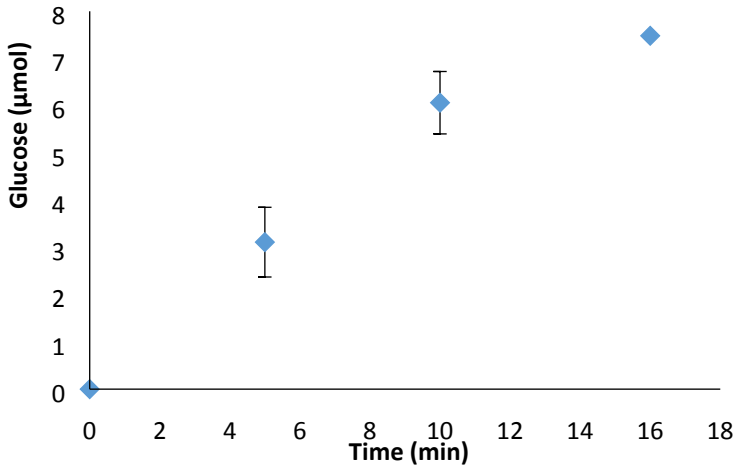

Figure S11. Reaction profiles for the hydrolysis of sucrose catalyzed by invertase covalently immobilized on RH.

S12. Immobilization of thermolysin on acrylic resin

A volume corresponding to 10 mg of protein per gram of carrier were loaded on ReliZyme EP403/S (Resindion, Binasco, Italy) in phosphate buffer 0.1M, pH 8.0. The immobilization was carried out at 35 °C per 24 h. Afterwards the biocatalyst was filtered and rinsed with phosphate buffer 0.02 M.

The activity resulted to be 5 Units per gram of biocatalyst and it was determined using casein as substrate, at 40 °C and pH 6.5. The reaction was made up of 5 mL casein 2% w v^{-1} and 1 mL of enzyme solution in phosphate buffer 0.1 M pH 6.5. The reaction was carried out at 40 °C for 15 min and stopped with 5 mL trichloroacetic acid. The absorbance of the supernatant was measured at 280 nm. One unit will hydrolyze casein to produce peptide equivalent to 1.0 µmol (181 µg) of tyrosine per minute at pH 6.5 and 40 °C.

Table S2: Preliminary evaluation of the greenness of RH as enzyme carrier

Compound	Full details on toxicity	Comments
Hexamethylenediamine	http://www.solvay.com/en/binaries/Hexamethylenediamine_GPS_rev0_sept12_RHD-139548.pdf	Hexamethylenediamine is considered as harmful to aquatic invertebrates, but as it is readily biodegradable and not potentially bioaccumulative, it is not classified as dangerous for the environment according to EU regulation (EC) 1272/2008. Bio-based routes for HMDA production are reported [*Green Chem*., 2015,17, 4760-4772].
Glutaraldehyde	H. W. Leung, Ecotoxicology of glutaraldehyde: review of environmental fate and effects studies, Ecotoxicol Environ Saf. 2001, 49, 26-3939 (2001)	Acutely toxic to aquatic organisms. The acute toxicity for avian species is comparable to that for mammalian species. Results from environmental partitioning studies indicate that glutaraldehyde tends to remain in the aquatic compartment and has little tendency to bioaccumulate. Glutaraldehyde is readily biodegradable in the freshwater environment and has the potential to biodegrade in the marine environment. Aquatic metabolism studies suggest that glutaraldehyde, under aerobic conditions, is metabolized to CO_2 via glutaric acid as an intermediate. Under anaerobic conditions, glutaraldehyde is metabolized to 1,5-pentanediol. Pretreatment with sodium bisulfite is the best method for inactivating glutaraldehyde prior to disposal to treatment systems.
Sodium periodate	http://www.sigmaaldrich.com/MSDS/MSDS/DisplayMSDSPage.do?country=IT&language=EN-generic&productNumber=311448&brand=SIAL&PageToGoToURL=http%3A%2F%2Fwww.sigmaaldrich.com%2Fcatalog%2Fproduct%2Fsial%2F311448%3Flang%3Dit	Classification according to Regulation (EC) No 1272/2008: • Oxidizing solids (Category 1), H271 • Skin corrosion (Category 1C), H314 • Specific target organ toxicity - repeated exposure (Category 1), thymus gland, H372 • Acute aquatic toxicity (Category 1), H400 Not considered to be either persistent, bioaccumulative and toxic. Not identified as probable, possible or confirmed human carcinogen by IARC. Acute toxicity: LD50 Intraperitoneal - Mouse - 58 mg/kg

.